

RESEARCH ARTICLE

# Human Parechovirus 1 Infection Occurs via $\alpha V\beta 1$ Integrin

Pirjo Merilahti, Sisko Tauriainen, Petri Susi\*

Department of Virology, University of Turku, Turku, Finland

\* [pesusi@utu.fi](mailto:pesusi@utu.fi)



OPEN ACCESS

**Citation:** Merilahti P, Tauriainen S, Susi P (2016) Human Parechovirus 1 Infection Occurs via  $\alpha V\beta 1$  Integrin. PLoS ONE 11(4): e0154769. doi:10.1371/journal.pone.0154769

**Editor:** Krzysztof Pyrc, Faculty of Biochemistry Biophysics and Biotechnology and Malopolska Centre of Biotechnology, Jagiellonian University, POLAND

**Received:** March 20, 2015

**Accepted:** April 19, 2016

**Published:** April 29, 2016

**Copyright:** © 2016 Merilahti et al. This is an open access article distributed under the terms of the [Creative Commons Attribution License](https://creativecommons.org/licenses/by/4.0/), which permits unrestricted use, distribution, and reproduction in any medium, provided the original author and source are credited.

**Data Availability Statement:** All relevant data are within the paper and its Supporting Information files.

**Funding:** This work was supported by Turku Doctoral Programme of Molecular Medicine, The Finnish Cultural Foundation, European Union (AIROPico, FP7-PEOPLE-2013-IAPP Grant no. 612308) (<http://airopico.eu>), Academy of Finland (grant no. 128539 to P.S.) ([www.aka.fi/en-GB/A/](http://www.aka.fi/en-GB/A/)) and Jane and Aatos Erkko Foundation (to S.T.). The funders had no role in study design, data collection and analysis, decision to publish, or preparation of the manuscript.

## Abstract

Human parechovirus 1 (HPeV-1) (family *Picornaviridae*) is a global cause of pediatric respiratory and CNS infections for which there is no treatment. Although biochemical and *in vitro* studies have suggested that HPeV-1 binds to  $\alpha V\beta 1$ ,  $\alpha V\beta 3$  and  $\alpha V\beta 6$  integrin receptor(s), the actual cellular receptors required for infectious entry of HPeV-1 remain unknown. In this paper we analyzed the expression profiles of  $\alpha V\beta 1$ ,  $\alpha V\beta 3$ ,  $\alpha V\beta 6$  and  $\alpha 5\beta 1$  in susceptible cell lines (A549, HeLa and SW480) to identify which integrin receptors support HPeV-1 internalization and/or replication cycle. We demonstrate by antibody blocking assay, immunofluorescence microscopy and RT-qPCR that HPeV-1 internalizes and replicates in cell lines that express  $\alpha V\beta 1$  integrin but not  $\alpha V\beta 3$  or  $\alpha V\beta 6$  integrins. To further study the role of  $\beta 1$  integrin, we used a mouse cell line, GE11-KO, which is deficient in  $\beta 1$  expression, and its derivative GE11- $\beta 1$  in which human integrin  $\beta 1$  subunit is overexpressed. HPeV-1 (Harris strain) and three clinical HPeV-1 isolates did not internalize into GE11-KO whereas GE11- $\beta 1$  supported the internalization process. An integrin  $\beta 1$ -activating antibody, TS2/16, enhanced HPeV-1 infectivity, but infection occurred in the absence of visible receptor clustering. HPeV-1 also co-localized with  $\beta 1$  integrin on the cell surface, and HPeV-1 and  $\beta 1$  integrin co-endocytosed into the cells. In conclusion, our results demonstrate that in some cell lines the cellular entry of HPeV-1 is primarily mediated by the active form of  $\alpha V\beta 1$  integrin without visible receptor clustering.

## Introduction

Integrins are heterodimeric transmembrane receptor proteins that mediate cell-cell and cell-extracellular matrix (ECM) interactions [1] often via a specific arginine—glycine—aspartic acid (RGD) motif. RGD-binding integrins include five  $\alpha V$  integrins ( $\alpha V\beta 1$ ,  $\alpha V\beta 3$ ,  $\alpha V\beta 5$ ,  $\alpha V\beta 6$ , and  $\alpha V\beta 8$ ), two  $\beta 1$  integrins ( $\alpha 5\beta 1$  and  $\alpha 8\beta 1$ ), and  $\alpha IIb\beta 3$  [2]. Human parechovirus 1 (HPeV-1) is one of the sixteen parechovirus types in the genus *Parechovirus* of the family *Picornaviridae* [3–15]. Parechovirus infections are commonly encountered during the first years of life and are often mild or asymptomatic [16–20]. However, besides gastroenteritis and respiratory infections, HPeV-1 causes infections of the central nervous system and severe generalized infections, as well as myocarditis especially in neonates [9,16,17,21,22]. The structure

**Competing Interests:** The authors have declared that no competing interests exist.

of a parechovirus is icosahedral, and like other picornaviruses, its genome is a positive-sense, single-stranded RNA molecule [23–25]. RGD motif resides on the surface of the HPeV-1 particle through which it interacts with cell surface integrin receptor(s) [26]. Among human picornaviruses, there are ten virus types that possess the RGD motif within the VP1 protein, but integrin binding has been shown experimentally only for coxsackievirus A9 (CV-A9), echovirus 9 (E-9), echovirus 1 (E-1), and HPeV-1 [26]. Remarkably, all cultivable parechoviruses with the exception of HPeV-3, possess the RGD motif suggesting that they all may bind and use integrin receptor(s) during infectious entry.

HPeV-1 has been shown to bind *in vitro* to  $\alpha V\beta 1$ ,  $\alpha V\beta 3$  and  $\alpha V\beta 6$  integrins [27–29], while it has been reported that during cellular infection HPeV-1 favors  $\alpha V\beta 3$  over  $\alpha V\beta 1$  integrin [29]. HPeV-1 receptor binding and use have often been compared to a related picornavirus, coxsackievirus A9 (CV-A9), which also bears the RGD motif [26,30]. Whereas CV-A9 can infect some cell lines devoid of the RGD motif or cells that do not express  $\alpha V$  integrins [31,32], HPeV-1 is more dependent on RGD-mediated integrin binding during cellular entry. After deletion of the RGD, the virus particles were essentially noninfectious, and only viruses in which the RGD sequence had been genetically restored were recovered [33]. We have recently shown that heparan sulfate possesses a role in HPeV-1 infection [34]. Another candidate receptor for HPeV-1 is matrix metalloproteinase 9 (MMP-9) [27], but these findings have not been corroborated by the others including us.

In the present study, we demonstrate that integrin  $\alpha V\beta 1$  plays a specific role in the infectious entry of HPeV-1 into A549, HeLa and SW480 cell lines. HPeV-1 did not bind to or internalize into  $\beta 1$  knock-out cell line (GE11-KO), whereas internalization into a cell line overexpressing  $\beta 1$  integrin (GE11- $\beta 1$ ) was successful. HPeV-1 co-localized with  $\beta 1$  integrin on the cell surface and co-internalized into the GE11 cells. Activation of  $\beta 1$  integrin affected HPeV-1 infectivity but integrin receptor clustering was not detected.

## Materials and Methods

### Cells, viruses, and antibodies

Human cervical cancer (HeLa-Ohio), human colorectal adenocarcinoma (SW480), and human lung carcinoma (A549) cell lines were from the American Type Culture Collection (ATCC). The  $\beta 1$  knockout cell line GE11-KO and its derivative  $\beta 1$  overexpressing cell line, GE11- $\beta 1$  (GE11- $\beta 1A$ ), were kind gifts from Arnoud Sonnenberg (The Netherlands Cancer Institute, The Netherlands) [35]. The cells were maintained in Dulbecco's modified Eagle Medium (DMEM) supplemented with 10% fetal calf serum (FCS) and gentamicin. In experiments where antibodies were used, DMEM was supplemented with 1 mM  $MgCl_2$ .

HPeV-1 (prototype, Harris strain) [3] and CV-A9 (prototype, Griggs strain) [30,36] were propagated in A549 cells and purified in sucrose gradients as described earlier [32]. Clinical HPeV-1 isolates with low passage numbers were from Dr. Katja Wolthers (Academic Medical Center, The Netherlands). The culture medium for virus infections was supplemented with 1% FCS, and the efficiencies of virus infections were determined with plaque titration assays.

The function blocking  $\beta 1$  integrin antibody 6S6 (MAb 2253) was from Millipore and the  $\beta 1$  integrin activating antibody TS2/16 (sc-53711) was from Santa Cruz. Other cell surface antibodies used were  $\alpha 5\beta 1$  (MAb 1969, Millipore) and  $\alpha V$  (L230, ATCC) which both are integrin function blocking antibodies. Fluorescence conjugated antibodies against  $\beta 1$  (303015) and  $\alpha V$  (327907) integrins, both from BioLegend, as well as unconjugated primary antibodies against  $\alpha V\beta 3$  (MAb 1976),  $\alpha V\beta 6$  (MAb 2077z) and  $\alpha 5\beta 1$  (MAb 1999), all from Millipore, were used in the flow cytometry analysis. Alexa Fluor (AF) 488-, 568- and 633-labeled anti-mouse and anti-rabbit secondary antibodies and 568-labeled phalloidin were from Life Technologies. Hoechst

33342 for staining nuclei was from Sigma-Aldrich. Samples for confocal microscopy were mounted with Prolong Gold anti-fade Reagent containing DAPI (Life Technologies). HPeV-1 and CV-A9 antisera were obtained by immunizing rabbits with sucrose gradient-purified viruses as described previously [37–39].

### Flow cytometry

Monoclonal antibodies were used to detect  $\alpha V$ ,  $\beta 1$ ,  $\alpha V\beta 3$ ,  $\alpha V\beta 6$  and  $\alpha 5\beta 1$  integrins on A549, HeLa and SW480 cell lines, and the expression level of  $\beta 1$  integrin was analyzed on GE11-KO and GE11- $\beta 1$  cells. The detached cells were suspended in the buffer solution (PBS containing 0.5% BSA), which was used throughout the experiment. Primary antibodies were added into the buffer and incubated for 1 h at 4°C. The cell pellets were washed and incubated with the secondary antibodies for 1 h at 4°C, and after washing the cells were suspended in the buffer. Flow cytometry measurements were done with a FACSCalibur flow cytometer (Becton Dickinson) and in total, 20 000 cells were analyzed in each experiment. The results were processed with a flow cytometry data analysis software (Flowing Software, [www.flowingsoftware.com](http://www.flowingsoftware.com)).

### HPeV-1 internalization and infectivity assays

Cells (A549, HeLa and SW480) were cultivated on 96-well plates (PerkinElmer) and inoculated with HPeV-1 at MOI of 10. After incubation for 1 h on ice, unbound viruses were removed, a pre-warmed infection medium was added, and the cells were transferred to a 37°C CO<sub>2</sub> incubator. After 6 h incubation, the cells were washed with PBS, fixed (15 minutes with 4% formaldehyde in PBS), permeabilized (10 minutes with 0.1% Triton-X100 in PBS) and stained (antibody dilutions were made in 3% BSA in PBS) with a virus-specific antiserum, and AF 488-labeled secondary antibodies at RT for 1.5 h. The nuclei were stained with Hoechst and infection efficiency was visualized by fluorescence microscope using a Zeiss Axiovert 200M (10 or 20× objective) (Zeiss).

### Antibody blocking assay

15  $\mu$ g/ml of function blocking antibodies in serum free DMEM, containing 1 mM MgCl<sub>2</sub>, were added onto confluent SW480 cells in 96-well plates and incubated for 1 h in RT with gentle shaking. Unbound antibodies were washed away with PBS and the cells were infected at MOI of 1 similarly as in the infectivity assay, stained with HPeV-1-specific antiserum and secondary antibody, and detected with a Zeiss Axiovert 200M (10× objective) microscope. The success rate (percentage of infected cells) was calculated with BioImageXD imaging software [40] ([www.bioimagexd.net](http://www.bioimagexd.net)) as described below. The cells infected in the absence of blocking antibodies were used as a mock control (100% infection), and the mean of duplicates of three experiments (more than 10 000 cells per antibody) was calculated. P-values were analyzed with paired t-test.

### Internalization of HPeV-1 and CV-A9 into GE11-KO and GE11- $\beta 1$ cells

GE11-KO and GE11- $\beta 1$  cells were grown on cover slips in 24-well plates and HPeV-1 (Harris), clinical HPeV-1 isolates, and CV-A9 (Griggs) as a control were inoculated onto cells. Viruses were incubated with the cells for 1 h on ice, after which unbound viruses were washed with PBS. Pre-warmed infection medium was added and incubated at 37°C for 6 h. The cells were washed, fixed and permeabilized as described above. For immunofluorescence labeling, the antibodies were diluted in PBS containing 3% BSA, and the cells were incubated with the antibodies at room temperature, primary antibodies for 1 hour and secondary antibodies for

30 minutes. The actin filament stain, phalloidin, was added with secondary antibodies to determine the borders of the cells. Following washing with PBS, the cells were mounted with ProLong Gold Antifade Reagent and examined with a Zeiss LSM780 confocal microscope using Plan-Apochromat objectives (63 $\times$  / 1.2 oil/water for HPeV-1 imaging, and 40 $\times$ / 1.2. oil/water for CV-A9 imaging).

### Activation of integrins

SW480 cells were treated with  $\beta$ 1 integrin activating antibody (TS2/16) at different concentrations (5  $\mu$ g, 20  $\mu$ g, and 50  $\mu$ g /ml) in 96-well plates and incubated at 37°C for 1 h. After incubation, HPeV-1 infection and virus staining was performed as described above in the infectivity assay. The samples were analyzed with a Zeiss Axiovert 200M (10 $\times$  objective) and BioImageXD software. The mock treated cells were used as a control (100% infection) and the mean was calculated from four parallel samples (20 000–40 000 cells/antibody concentration). P-values were analyzed with paired t-test.

### Integrin clustering

SW480 cells were grown on cover slips in 24-well plates. The experimental procedure was performed as described in echovirus 1 studies [41,42]. Samples included 1) a negative control for clustering, where cells were incubated only with primary  $\beta$ 1 integrin antibody (TS2/16) followed by fixing and staining with a secondary antibody and DAPI, 2) a positive control for clustering, where cells were first incubated with  $\beta$ 1 integrin antibody, after which the secondary antibody was added to induce  $\beta$ 1 integrin clustering, followed by fixing and DAPI staining, and 3) a virus sample, where cells were incubated with HPeV-1 for 15 minutes followed by fixing and staining (anti-HPeV-1, anti- $\beta$ 1 integrin antibodies and DAPI for staining nuclei). The samples were examined with a Zeiss LSM780 confocal microscope using a Plan-Apochromat objective (63 $\times$  / 1.2 oil/water).

### HPeV-1 co-localization with $\beta$ 1 integrin in GE11- $\beta$ 1 cells

To test HPeV-1 co-localization with  $\beta$ 1 integrin, GE11- $\beta$ 1 cells were inoculated with HPeV-1 at MOI of 5. After 1 h on ice, unbound viruses were removed, a pre-warmed infection medium was added, and the cells were transferred to 37°C where the infection was followed. After specific time points (0, 5 and 30 minutes post infection) the cells were washed, fixed and permeabilized. However, the 0-min sample was not permeabilized because the co-localization was analyzed from the cell surface only. The samples were stained as described earlier and examined with a Zeiss LSM780 confocal microscope using a Plan-Apochromat objective (63 $\times$  / 1.2 oil/water). Co-localization analyses (automatic thresholding after background subtraction, Costes P-value calculation with 100 iterations) of selected image stacks were performed with BioImageXD software [40].

### BioImageXD analysis

The calculation of infection efficiency was analyzed with BioImageXD software [40]. Image datasets taken with Zeiss Axiovert 200M were imported and the total number of cells (blue channel, nuclei) and infected cells (green channel, HPeV-1) were calculated separately, after which the percentage of infection was calculated manually. The settings were set on the basis of control cells, and image threshold was set to make all cells visible based on staining of nuclei (blue channel). The number of objects was then automatically calculated. The analysis was performed in the same way for the infected cells but in this case a green channel was used

indicating only the cells positive for virus staining. The percentage of infections was calculated manually after determining the numbers of infected and total cell count.

## Results

### HPeV-1 infects cells in the absence of integrin $\alpha V\beta 3$ and $\alpha V\beta 6$

Previous studies indicate that both human parechovirus 1 (HPeV-1) and a related enterovirus, coxsackievirus A9 (CV-A9), bind to integrin  $\alpha V\beta 3$  and  $\alpha V\beta 6$  *in vitro* [28,31,43–45]. It has also been suggested that HPeV-1 may use either  $\alpha V\beta 1$  or preferentially  $\alpha V\beta 3$  integrin as cellular receptor [29]. To elucidate the role of integrin  $\alpha V\beta 1$ ,  $\alpha V\beta 3$ , and  $\alpha V\beta 6$  in HPeV-1 infection *in vivo*, the receptor tropism of HPeV-1 in three cell lines, A549, HeLa, SW480, was examined.

Firstly, we determined the susceptibility of these three cell lines for HPeV-1 infection. The cells were infected at MOI of 10, washed after one hour binding on ice, and the infection was followed for six hours before staining with HPeV-1 specific antiserum. The infection was visualized by immunofluorescence microscopy, and the results show that HPeV-1 internalizes and infects these cell lines efficiently (Fig 1A). Secondly, we performed a flow cytometry analysis which showed, as expected, that A549 cells express integrin subunits  $\alpha V$  and  $\beta 1$  as well as integrin  $\alpha V\beta 3$  and  $\alpha V\beta 6$  while expression of  $\alpha V\beta 3$  and  $\alpha V\beta 6$  is not detected on HeLa and SW480 cells (Fig 1B). All three cell lines highly express integrin  $\alpha 5\beta 1$ . Both  $\alpha V$  and  $\beta 1$  are shown on the cell surface with high levels suggesting that integrin  $\alpha V\beta 1$  is available for virus binding. The visualization of the  $\alpha V\beta 1$  heterodimer was performed with subunit specific antibodies because specific antibodies against integrin  $\alpha V\beta 1$  are not commercially available. The results indicated that irrespective of the integrin expression profile, all these cell lines supported HPeV-1 replication based on the immunofluorescence images and RT-qPCR at 1 h and 6 h time points (S1 Fig). No virus was visualized at 0 h and 1 h time points whereas virus accumulation was evident at 6 h time point. This suggested that neither  $\alpha V\beta 3$  nor  $\alpha V\beta 6$  is required for efficient HPeV-1 infection into A549, HeLa and SW480 cells.

### HPeV-1 utilizes $\alpha V\beta 1$ integrin in human epithelial colon carcinoma cell line

We and others have used a human epithelial colon carcinoma SW480 cell line in CV-A9 infection studies, and shown that CV-A9 infection proceeds independent of  $\alpha V$  integrin [45]. Because HPeV-1 and CV-A9 have similar *in vitro* integrin-binding properties [28,31], the dependency of HPeV-1 on  $\alpha V$  integrin was studied further by using integrin function-blocking antibodies (Fig 2). SW480 cells were blocked with  $\alpha V$  and  $\beta 1$  integrin antibodies and with  $\alpha 5\beta 1$  integrin antibody. Currently, commercial  $\alpha V\beta 1$  specific antibodies are not available, and therefore anti- $\alpha V$  and anti- $\beta 1$  antibodies were used separately and in combination. Cells were incubated with function blocking antibodies prior to HPeV-1 infection, stained, and imaged with a fluorescence microscope. Relative percentages of HPeV-1 infections were calculated using BioImageXD software (Fig 2), and infection efficiency of mock treated SW480 cells was set to 100 percent. As shown in Fig 2B, there was 70% ( $p = 2.66 \times 10^{-4}$ ) and 60% ( $p = 7.37 \times 10^{-4}$ ) reduction in relative infection efficiency in anti- $\alpha V$  and anti- $\beta 1$  antibody-blocked cells, respectively, compared to non-blocked control, while the combined effect of  $\alpha V$  and  $\beta 1$  antibodies resulted in almost 80% ( $p = 3.07 \times 10^{-7}$ ) reduction in HPeV-1 infectivity. Because  $\alpha 5\beta 1$  integrin is also capable of binding the RGD motif and functions similarly to  $\alpha V\beta 1$  [46], its ability to block HPeV-1 was also tested. The reduction caused by the blocking  $\alpha 5\beta 1$  integrin antibody was in the range of 20%, which suggests together with the other data

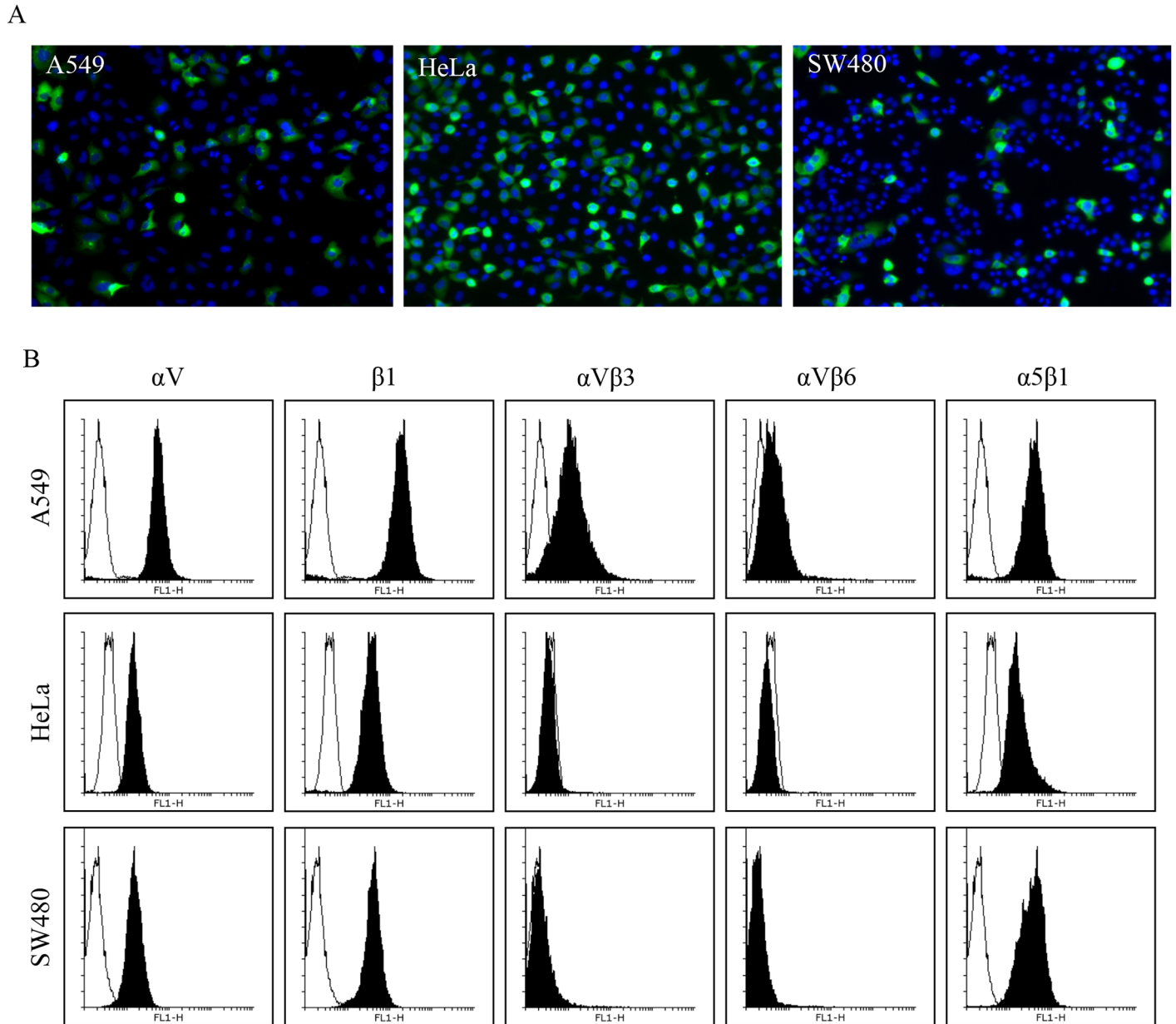


**Fig 1. HPeV-1 infects the cell lines that do not express  $\alpha V\beta 3$  and  $\alpha V\beta 6$  integrins.** (A) A549, HeLa, and SW480 cell lines were inoculated with HPeV-1 at MOI of 10, unbound viruses were removed followed by incubation at 37°C for 6 h, and processed for immunofluorescence staining and imaging (with a 20x objective). HPeV-1 particles and nuclei are shown in green and blue, respectively. (B) The receptor profile of A549, HeLa and SW480 cells was analyzed with flow cytometry. Cells were fixed, and cell surface integrins ( $\alpha V$ ,  $\beta 1$ ,  $\alpha V\beta 3$ ,  $\alpha V\beta 6$  and  $\alpha 5\beta 1$ ) were stained using specific antibodies, and 20 000 cells/antibody was measured by flow cytometry.

doi:10.1371/journal.pone.0154769.g001

that integrin  $\alpha\beta 1$ , and not  $\alpha 5\beta 1$ , is the principal receptor for infectious entry of HPeV-1 into SW480 cell line.

### $\beta 1$ integrin is required for HPeV-1 internalization into GE11 cells

Previous studies with receptor use of HPeV-1 have been performed either using purified integrins in *in vitro* experiments [28], or by measuring virus binding to cell surface using cell sorting

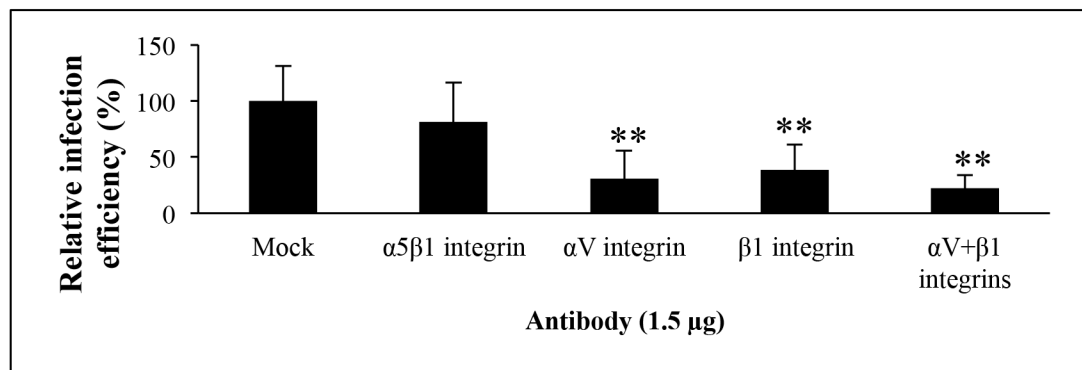
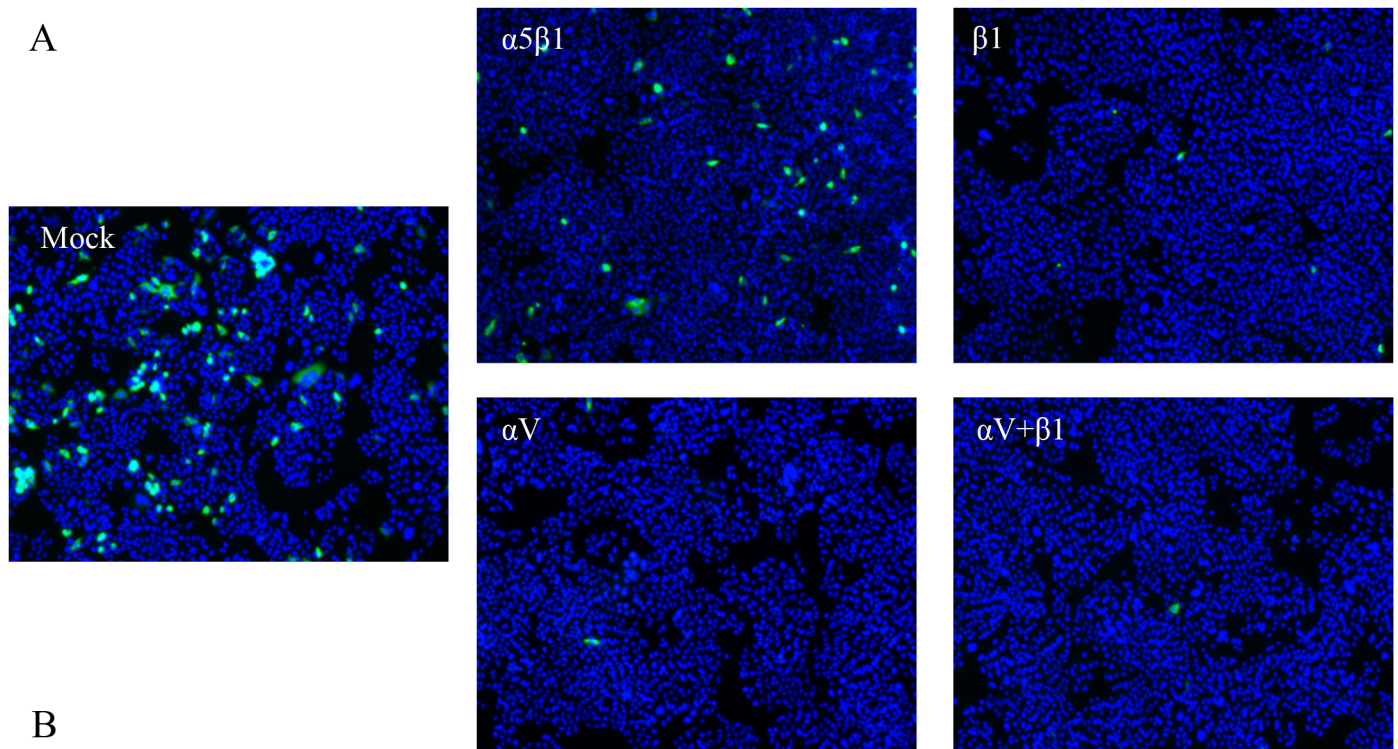


**Fig 2. HPeV-1 infection is inhibited by integrin function-blocking antibodies.** (A) Immunofluorescence microscopy of antibody-treated SW480 cells infected with HPeV-1. SW480 cells were treated with 15  $\mu$ g/ml of anti-integrin antibodies for 1 h and subsequently infected with HPeV-1 at a MOI of 10. The cells were incubated with HPeV-1 for 1 h on ice followed by wash and incubation for 6 h at 37°C. The cells were fixed and stained with nuclear stain Hoechst (blue) and HPeV-1 specific antiserum (green). (B) Relative infection efficiency of HPeV-1 in integrin-treated cells. SW480 cells were processed as in Fig 2A. The infection efficiency of HPeV-1 in total of 10 000 cells was counted from microscopic images, and p values were calculated. Percentage of HPeV-1 infection in mock-treated (control) cells was set as 100%. Standard deviations are shown, and \*\* indicates  $p < 0.001$ . The cells were imaged with a 10 $\times$ objective.

doi:10.1371/journal.pone.0154769.g002

and immunoprecipitation techniques [29,44]. It can be speculated whether *in vitro* binding represents the actual situation during dynamic cellular infection, whereas cell sorting experiments do not exclude the possibility that other receptors than integrins are included in the entry process. We therefore used a knock-out cell line to examine the use of  $\beta$ 1 integrin as the receptor of HPeV-1 [35]. The HPeV-1 infectivity assay was performed in a mouse epithelial cell line, GE11-KO, with genetic knock-out of  $\beta$ 1 gene [35]. As a control, the same cell line

overexpressing the  $\beta 1$  subunit, GE11- $\beta 1$  [35], was used (Fig 3A). The expression of  $\beta 1$  integrin was confirmed by flow cytometry (Fig 3A, right panel) and also by staining, shown in blue in Fig 3A. Virus internalization into the GE11- $\beta 1$  cell line was visualized by confocal microscopy, which allowed the detection of the virus within cell interior. S2 and S3 Figs show confocal slices of internalized HPeV-1 at 6 h and 24 h time points suggesting that virus accumulates but does not replicate or cause cytopathic effect in GE11- $\beta 1$  cells. The data suggest that  $\beta 1$  integrin is essential for internalization of HPeV-1 into GE11- $\beta 1$  cells.

We also tested the cellular tropism of three HPeV-1 clinical isolates, because it is possible that the HPeV-1 prototype (Harris strain), which dates back to 1950s, may not possess the characteristics of the recent HPeV-1 isolates. As shown in Fig 3B, the clinical isolates internalized into GE11- $\beta 1$  but not into GE11-KO cells similarly to HPeV-1 Harris strain. We also showed that CV-A9 is capable of infecting both GE11-KO and GE11- $\beta 1$  cells (Fig 3C), which is basically the first indication that these viruses have different cellular receptor tropism even though they have been shown to have similar *in vitro* binding properties to integrin  $\alpha V\beta 3$  and  $\alpha V\beta 6$  [28,31]. CV-A9 is clearly visible in the cytoplasm indicating that CV-A9 can replicate in these cell lines but this was not tested further. Although HPeV-1 cannot infect GE11- $\beta 1$  cell line, the  $\beta 1$  integrin enables the HPeV-1 internalization. In the light of these findings, the data support the view that human  $\beta 1$  integrin possibly paired to mouse  $\alpha V$  is sufficient to support HPeV-1 internalization in GE11 cells.

## Integrin activation mediates HPeV-1 infection without visible receptor clustering

Integrin activation is a controlled procedure by which the cell regulates ligand binding to integrins. It is sometimes followed by integrin receptor clustering, which is considered to be an important mechanism for generation of intracellular signals required for virus entry. The activation is known to be bi-directional: either from outside-in or inside-out. Extracellular domains of integrins are known to possess different conformations, which are highly dependent on the integrin type [47]. Previously, activating  $\beta 1$  integrin antibody TS2/16 has been shown to increase the entry rate of adenovirus 5 (Ad5) [48]. We used TS2/16 antibody to analyze the effect of integrin conformation on HPeV-1 infection and to test whether HPeV-1 infection is affected by integrin activation. SW480 cells were incubated for 1 h with different concentrations of TS2/16 antibody followed by HPeV-1 infection and staining. The cells were visualized by immunofluorescence microscopy (Fig 4A) and relative infectivity was measured from 20 000 to 40 000 cells with BioImageXD software. Infection of mock treated SW480 cells was set to 100 percent. Increasing the amount of activating  $\beta 1$ -antibody increased the infectivity by 2.5-fold (Fig 4B). 0.5  $\mu\text{g}$  of TS2/16 antibody increased infection to 170% ( $p = 1.96 \times 10^{-3}$ ), 2  $\mu\text{g}$  to 210 percent ( $p = 6.59 \times 10^{-5}$ ) and 5  $\mu\text{g}$  to 250% ( $p = 9 \times 10^{-7}$ ) when compared to control. This indicates that the activation of  $\beta 1$  integrin affects HPeV-1 internalization and infection.

We also examined whether virus binding to cell surface induced integrin receptor clustering. Effective clustering of integrins has been demonstrated earlier with echovirus 1 (E-1, an enterovirus) [41,42], and we used the same protocol to study the clustering of  $\beta 1$  integrins during HPeV-1 infection (Fig 4C). A positive control, where  $\beta 1$  integrins have been clustered with  $\beta 1$  primary and secondary antibody prior to fixing, is shown on the left panel. HPeV-1 infected cell is shown in the middle, and a negative control where cells were incubated only with  $\beta 1$  antibody prior to fixing and staining is shown on the right. The  $\beta 1$  antibody-induced integrin clusters are clearly visible as bright spots around the cell. The infection of cells with HPeV-1 does not induce clear  $\beta 1$  integrin clustering, which is visible during E-1 infection [41,42]. The pattern of  $\beta 1$  integrins in infected cells looks similar to negative controls, where integrins are



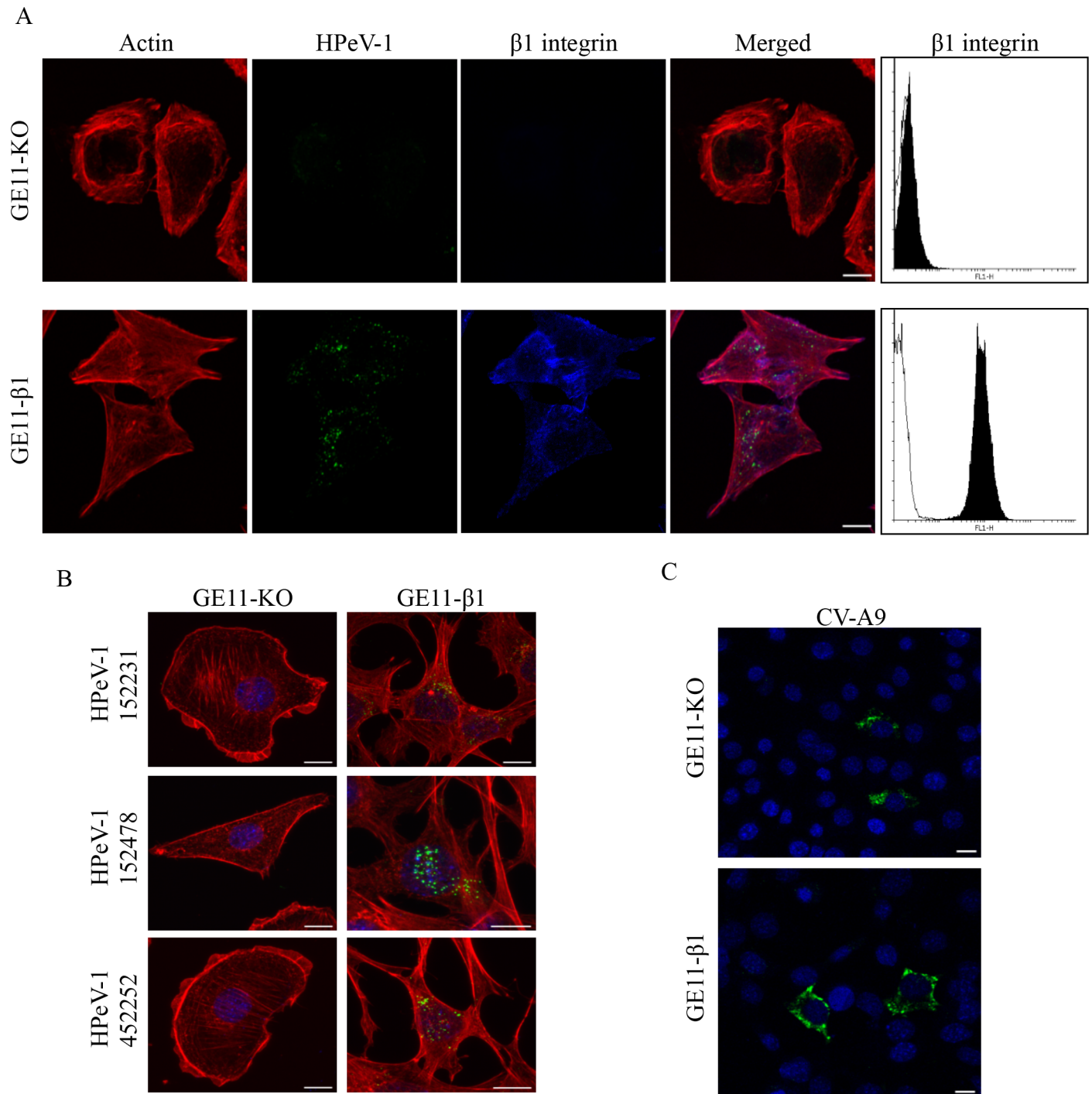


**Fig 3. HPeV-1 internalization is inhibited in mouse cells lacking  $\beta$ 1 integrin expression.** (A) HPeV-1 internalizes into GE11- $\beta$ 1 but not GE11-KO cells. GE11-KO and - $\beta$ 1 cells were inoculated with HPeV-1 at a MOI of 5 on ice for 1 h followed by incubation for 6 h at 37°C. The cells were fixed, permeabilized, and stained with appropriate stains or antibodies as described in Materials and Methods. Actin filaments are shown in red, HPeV-1 in green and  $\beta$ 1 integrin in blue. The  $\beta$ 1 integrin expression on the cell surface was also analyzed by flow cytometry (right panel). (B) Clinical HPeV-1 isolates with low passage numbers (152231, 152478 and 452252) act similarly to the prototype. The cells were treated as in (A). (C) CV-A9 infects both GE11-KO and GE11- $\beta$ 1 cells. The CV-A9 infection was performed similarly to the HPeV-1 assay, followed by staining with anti-CV-A9 antibody (green) and DAPI (blue). Microscopic imaging was performed with Zeiss LSM780 confocal microscopy using a Plan-Apochromat objectives (63x / 1.2 oil/water [panels A and B] or with 40x / 1.2. oil/water [panel C]). Bar 10  $\mu$ m.

doi:10.1371/journal.pone.0154769.g003

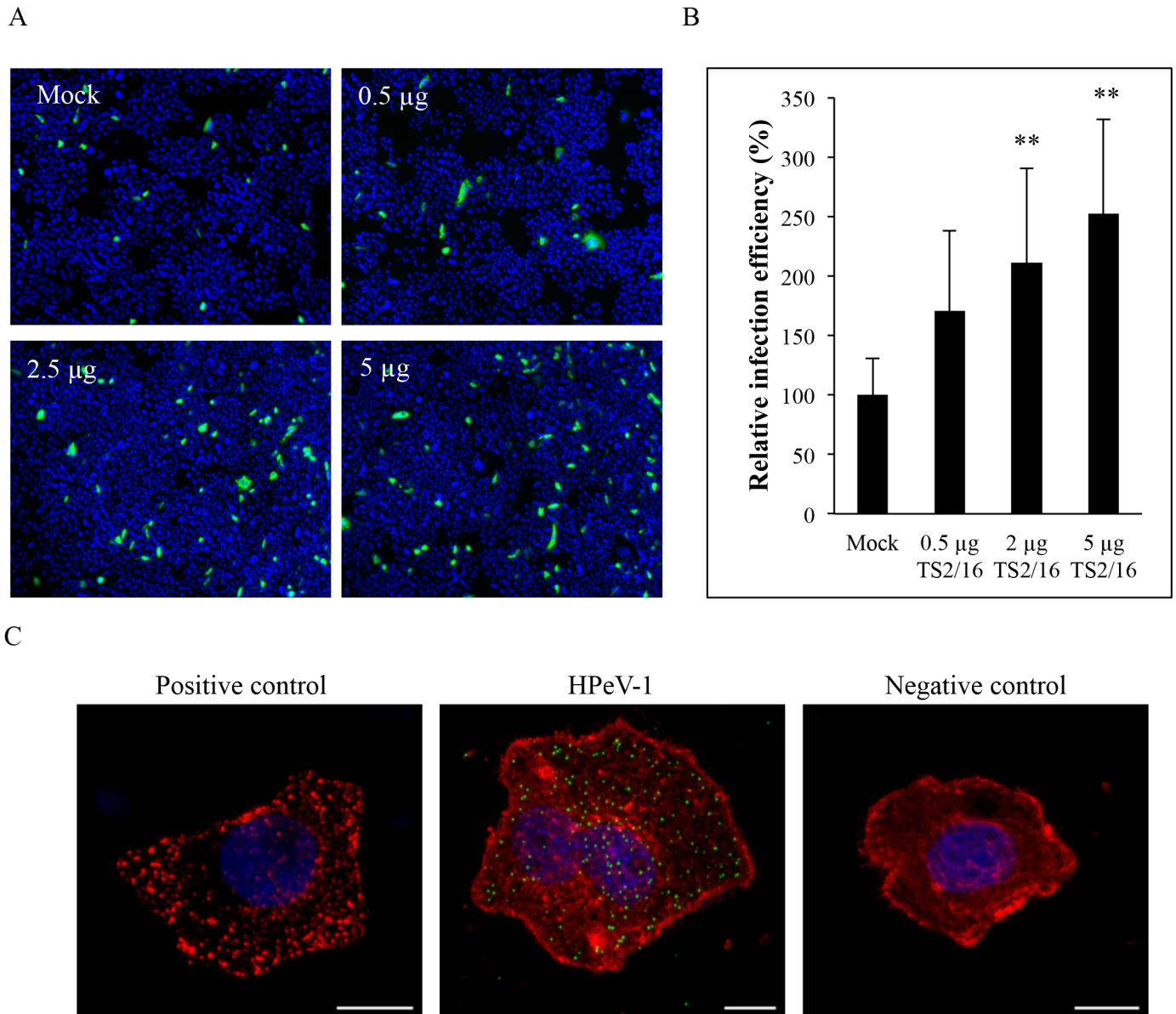


**Fig 4. Activation of  $\beta 1$  integrins enhances HPeV-1 infectivity without visible receptor clustering.** (A and B) SW480 cells were treated with  $\beta 1$  integrin activating antibody (TS2/16) at 37°C for 1 h after which the cells were inoculated on ice with HPeV-1 at a MOI of 10 followed by incubation for 6 h at 37°C. The cells were fixed, permeabilized and stained. The relative infection efficiency of HPeV-1 was calculated from nine parallel images (totally 20 000 to 40 000 cells per each antibody concentration) obtained with Zeiss Axiovert 200M (10 $\times$ objective). The percentage of infection of HPeV-1 in mock-treated (control) cells was set as 100%. The error bars indicate standard deviation, \* indicates  $p < 0.01$  and \*\* indicates  $p < 0.001$ . (C) Receptor clustering is not detected during HPeV-1 infection in SW480 cell line. The cells were incubated with activating anti- $\beta 1$  antibody for 15 min after which a secondary antibody was added, and incubation was continued for another 15 minutes before fixing of the cells (positive control, left panel). HPeV-1 was allowed to bind to SW480 cells for 15 minutes before fixing and staining (middle panel). SW480 cells were incubated with  $\beta 1$  primary antibody for 15 minutes prior to fixation of the cells. Integrin  $\beta 1$  is shown in red, HPeV-1 in green and nuclei in blue. Microscopic imaging was performed using Zeiss LSM780 confocal microscopy using a Plan-Apochromat objective (63 $\times$  / 1.2 oil/water). Bar 10  $\mu\text{m}$ .

doi:10.1371/journal.pone.0154769.g004

not clustered. However, it is possible that HPeV-1 causes small microclusters [49] that are not detectable at the resolution of light microscopy. It should be noted that because the cells were not permeabilized all visualized integrins and viruses are located on the cell surface and not inside the cell. The results showed that in SW480 cells, HPeV-1 does not lead to macroclustering of  $\beta 1$  integrins although virus infectivity is enhanced by the receptor activating antibodies.

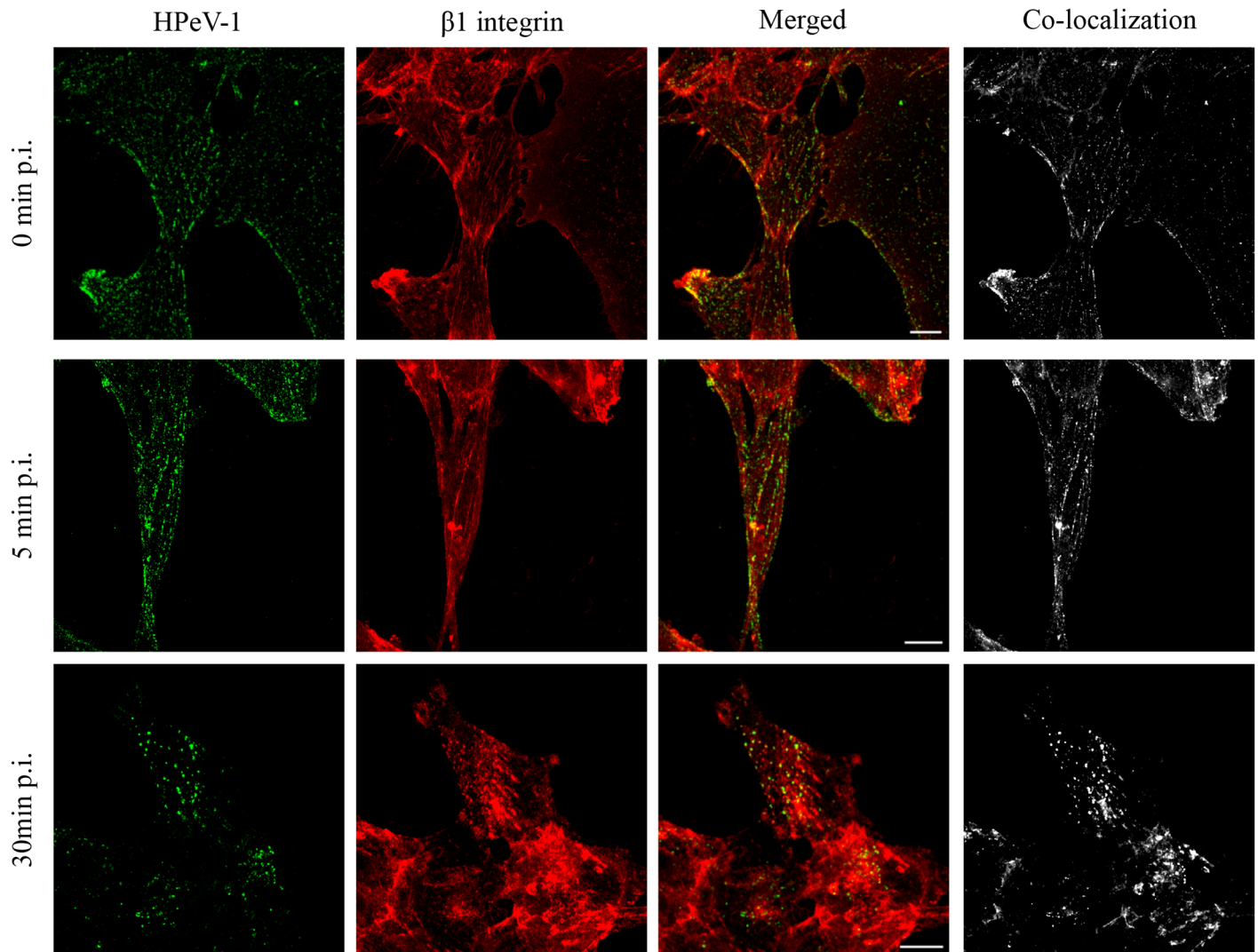


**Fig 5. HPeV-1 co-localizes with  $\beta$ 1 integrin during the early stages of virus entry.** GE11- $\beta$ 1 cells were inoculated on ice for 1 h with HPeV-1 at a MOI of 5 and incubated for 0 (non-permeabilized), 5 and 30 minutes (permeabilized) at 37°C before fixing and staining. HPeV-1 is shown in green and  $\beta$ 1 integrin in red. The right panel shows the co-localization analysis performed by BioImageXD software. The software calculates co-localizing voxels between two channels (HPeV-1 and  $\beta$ 1 integrin), and these (co-localizing voxels) are shown in white. Microscopic imaging was performed with Zeiss LSM780 confocal microscopy using a Plan-Apochromat objective (63 $\times$  / 1.2 oil/water). Bar 10  $\mu$ m.

doi:10.1371/journal.pone.0154769.g005

### HPeV-1 co-localizes with $\beta$ 1 integrin during early stages of entry

Successful HPeV-1 internalization in cell lines devoid of  $\alpha$ V $\beta$ 3 and  $\alpha$ V $\beta$ 6 integrins and in integrin  $\beta$ 1 knock-out cell line overexpressing  $\beta$ 1 suggested that HPeV-1 primarily uses the  $\alpha$ V $\beta$ 1 integrin during cellular infection. In GE11- $\beta$ 1 cells, HPeV-1 co-endocytose with  $\beta$ 1 integrin during internalization and early stages of entry (Fig 5). We further analyzed co-localizations with BioImageXD software, which allows mathematical analysis of co-localization points, and thus gives more objective interpretation of the confocal images than visual inspection. The analyses with BioImageXD indicated that almost every virus particle was interacting with  $\beta$ 1 integrin. This is illustrated in the right panel of Fig 5 in which all co-localizing voxels,

which are located exactly in the same place in the sliced image, are shown in white. We also calculated Manders' coefficient values (M1) of HPeV-1 co-localization to  $\beta 1$  integrin with BioImageXD. M1 values are proportional to the amount of fluorescence of the co-localizing objects in each component of the image, relative to the total fluorescence in that component. When  $M = 1.0$ , co-localization is fully achieved [50]. M1 of HPeV-1 infected samples were 1.0 (0 min), 0.84 (5 min), and 1.0 (30 min),  $P = 1.0$ . These data confirm that HPeV-1 binds to and is co-internalized with  $\alpha V\beta 1$  integrin.

## Discussion

Previously, human parechovirus 1 (HPeV-1) has been shown to interact with integrin  $\alpha V\beta 1$ ,  $\alpha V\beta 3$ , or  $\alpha V\beta 6$  in *in vitro* binding assays or in a cryoEM reconstruction [28,29]. It has also been reported that during cellular infection HPeV-1 favors  $\alpha V\beta 3$  over  $\alpha V\beta 1$  integrin [29]. In this work, we analyzed the receptor-mediated internalization and infectious entry of HPeV-1 into A549 (human lung carcinoma), HeLa (human cervical cancer), SW480 (human colorectal adenocarcinoma), and mouse epithelial GE11 cell lines, and found that HPeV-1 internalized into cell lines that do not express integrin  $\alpha V\beta 3$  and  $\alpha V\beta 6$ . Instead,  $\alpha V\beta 1$  integrin was shown to be essential for HPeV-1 entry.

To demonstrate the importance of  $\beta 1$  integrin in HPeV-1 internalization and infection, we used a  $\beta 1$ -deficient mouse epithelial cell line GE11-KO [35]. Both prototype and clinical HPeV-1 isolates internalized into  $\beta 1$  overexpressing GE11 cells (GE11- $\beta 1$ ), but not to GE11-KO. Thus, even if HPeV-1 did not replicate in GE11- $\beta 1$  cells (S3 Fig), it is evident that  $\beta 1$  integrin is needed for efficient internalization of the virus. Previous study has shown that  $\alpha V$  subunit, which is highly expressed in GE11- $\beta 1$  cell line, pairs with  $\beta 1$  and  $\beta 5$  subunits [51]. However, it is unlikely that HPeV-1 uses  $\alpha V\beta 5$  as cellular receptor, because it does not support HPeV-1 infection in A549 cells [29]. An interesting result in our experiments was that whereas CV-A9 was capable of internalizing GE11-KO and GE11- $\beta 1$  cell lines, HPeV-1 was not, which is basically the first demonstration that these viruses possess differential cellular receptor tropism. Previously, these viruses have been shown to have very similar *in vitro* binding properties to integrin  $\alpha V\beta 3$  and  $\alpha V\beta 6$  [28,31]. Both CV-A9 and HPeV-1 possess the RGD motif in the C-terminus of VP1 capsid protein [26,28,36], but only CV-A9 can infect cells even RGD motif was genetically removed [31]. However, the receptor for RGD-independent entry of CV-A9 remains unknown. In the light of the current findings it can be debated what is the actual role of RGD-binding integrins in the infectious entry of both CV-A9 and HPeV-1.

The observation that HPeV-1 internalizes into cells association with  $\beta 1$  integrin further supports the role of  $\beta 1$  as HPeV-1 receptor. At the zero time point, HPeV-1 co-localized completely with  $\beta 1$  integrin on the cell surface. Furthermore, HPeV-1 internalized into cells expressing  $\beta 1$  integrin, and these virus-integrin complexes accumulated in intracellular vesicles 30 minutes post-infection. To further demonstrate the specific role of  $\beta 1$  integrin in HPeV-1 infection, we used a  $\beta 1$  integrin activating monoclonal antibody, TS2/16, to activate  $\beta 1$  integrins. The activation of  $\beta 1$  integrins using this antibody prior to infection increased HPeV-1 infectivity, and this demonstrated that the virus may prefer the activated form of  $\beta 1$  integrin in cellular entry. This is different from echovirus 1 (E-1), which has been shown to bind to closed, non-activated, conformation of  $\alpha 2\beta 1$  [42]. Few other human viruses have also been reported to bind inactive integrin [52–55], but besides Adenovirus 5 (Ad5) [48], there seems to be no other human virus than HPeV-1 that specifically utilizes activated integrins in the cellular entry. However, binding of a related aphtovirus (within *Picornaviridae* family), Foot-and-mouth disease virus (FMDV), to  $\beta 1$  integrin has been shown to be affected by manganese ions and  $\beta 1$  integrin activating antibody 9EG7 [56]. Usually the activation of integrins induces intracellular

signaling [1]. Virus-induced integrin signaling has been studied previously with few viruses, including cytomegalovirus [57–59], adenoviruses [60–62], herpesviruses [63,64], echovirus 1 [41,42,65], and coxsackievirus A9 [32]. It can be speculated that binding of HPeV-1 to active conformation of  $\alpha V\beta 1$  integrin mimics the binding of its natural ligands (fibronectin and vitronectin). However,  $\alpha V\beta 1$  integrin binding to its natural ligands occurs relatively weakly [46,66], which may provide HPeV-1 the opportunity to bind to its integrin receptor with higher affinity (or avidity) than their ligands, and this may increase the rate of infection.

One of the key events in virus-receptor interactions is the clustering of receptors, which may lead to signaling cascade facilitating virus internalization. It has not been demonstrated previously whether HPeV-1 binding to any integrin receptor induces clustering and cellular signaling. We used the anti- $\beta 1$  TS2/16 antibody, because the same antibody could be used in both clustering of integrins and visualization of the cell-bound virus, i.e. the antibody did not interfere with virus binding to the  $\beta 1$  receptor. We did not see any integrin  $\beta 1$  clustering on the cell surface at the early stages (0 or 5 min p.i.) of HPeV-1 internalization. This suggested that HPeV-1 does not need to induce visible integrin clusters to be internalized. Integrin  $\alpha V\beta 1$  has been reported to localize predominantly diffused, and not in focal contacts, indicating that it does not interact with cytoskeletal proteins in the same manner as for example  $\alpha 5\beta 1$  integrin [46]. The fact that  $\alpha V\beta 1$  is randomly distributed in the cell instead of being clustered at specific locations may explain why HPeV-1 does not induce visible clusters (macroclusters) although we cannot exclude the possibility of microclustering. Our findings are opposite to E-1, an enterovirus, which binds to non-activated  $\alpha 2\beta 1$  integrin and induces clear receptor clustering [41,42]. Integrin clustering has also been studied with few other viruses. Studies with Ad5 have revealed that the location of RGD on penton protein affects virus binding to its integrin receptor ( $\alpha V\beta 3$ ) with subsequent clustering prior to internalization [67]. On the other hand, CV-A9 did not induce clustering of  $\alpha V\beta 6$  integrins during cell entry [32]. Recently, Vaccinia virus (VV) was shown to internalize into HeLa and GD25 cells via  $\beta 1$  integrin and by activating the PI3K/Akt signaling pathway [68], but it is not known if clustering was involved. Further studies are needed to elucidate the interplay between the lack of clustering and possible signaling events due to binding of HPeV-1 to (activated) integrin  $\alpha V\beta 1$ .

Here, we suggest that HPeV-1 uses  $\alpha V\beta 1$  integrin, instead of  $\alpha V\beta 3$  and  $\alpha V\beta 6$  integrins, for cell internalization and cellular infection. Integrins are used as receptors by several viruses [69], and  $\alpha V\beta 1$  acts as a receptor for HPeV-1 and a few other viruses. Human metapneumovirus (hMPV) and Foot-and-mouth-disease virus (FMDV) utilize  $\alpha V\beta 1$  integrin [56,70], and Ad5 uses  $\alpha V\beta 1$  integrins as well as many other integrins as its receptors [48,71]. Integrin  $\alpha V\beta 1$  is also commonly expressed in many cancerous cell lines, and therefore it will be of interest to determine whether cancer cell lines other than those used in this study express  $\alpha V\beta 1$  and are susceptible to HPeV-1 infection [72,73]. In this regard, infection of HPeV-1 via  $\beta 1$  integrin suggests that it may be useful in oncolytic virotherapy. For example, human melanoma, breast cancer, and neuroblastoma cells highly express  $\alpha V\beta 1$  integrin [74–76], and these cells may be susceptible to cytolytic infection by HPeV-1. It remains to be determined whether small molecular compounds developed against integrin  $\beta 1$  and used in cancer therapy prove to be protective against parechoviral disease.

## Supporting Information

**S1 Fig. Infectivity assay controls.** A549 control cells were treated, stained and imaged similarly to the other samples (Figs 1 and 2), but they were fixed at 0 min time point (A), 1 h time point (B) and 6 h time point (C). Control image (A) was negative for virus staining, which confirms that all green color in other images arises from internalized or newly-formed virus

particles. At 1 h time point (B) was no visible staining, but at 6 h time point (C) green staining indicates replicated virus.

(PDF)

**S2 Fig. A single slice from stacked confocal image (from the Fig 3A).** Virus particles shown in green are visible in the cell interior confirming that HPeV-1 internalizes the GE11- $\beta$ 1 cells.

(PDF)

**S3 Fig. HPeV-1 in GE11- $\beta$ 1 cells at 24 h post-inoculation.**

(PDF)

**S1 Table. Detection of HPeV-1 at 1 h and 6 h time points by RT-qPCR.** Results are presented as the mean of Ct values from two parallel samples in the same run. In average, 3.3 difference in Ct values equals to 10-fold difference in the RNA amount in the original sample.

(PDF)

## Acknowledgments

We gratefully acknowledge the technical assistance of Ms. Ritva Kajander and Mrs. Marja-Leena Mattila. Dr. Katja Wolthers (Amsterdam Medical Centre, The Netherlands) is thanked for clinical HPeV-1 isolates. GE11 cells were a kind gift from Dr. Arnoud Sonnenberg (The Netherlands Cancer Institute, Amsterdam, Netherlands). Cell imaging was performed in Turku Cell Imaging Core (Turku Centre for Biotechnology). Co-localization analyses were performed by Ms. Silja Tiitta (University of Turku). This work was supported by Turku Doctoral Programme of Molecular Medicine, The Finnish Cultural Foundation, European Union (AIR-OPico, FP7-PEOPLE-2013-IAPP Grant no. 612308), Academy of Finland (grant no. 128539 to P.S.) and Jane and Aatos Erkkö Foundation (to S.T.). We thank Michael Nelson (University of Turku Language Centre, Turku, Finland) and Mrs. Elli Sillanpää (Turku University of Applied Sciences) for the language revision.

## Author Contributions

Conceived and designed the experiments: PM ST PS. Performed the experiments: PM. Analyzed the data: PM PS. Contributed reagents/materials/analysis tools: ST PS. Wrote the paper: PM ST PS.

## References

1. Hynes RO. Integrins: bidirectional, allosteric signaling machines. *Cell*. 2002; 110: 673–687. PMID: [12297042](#)
2. Humphries JD, Byron A, Humphries MJ. Integrin ligands at a glance. *J Cell Sci*. 2006; 119: 3901–3903. PMID: [16988024](#)
3. Hyypia T, Horsnell C, Maaronen M, Khan M, Kalkkinen N, Auvinen P, et al. A distinct picornavirus group identified by sequence analysis. *Proc Natl Acad Sci U S A*. 1992; 89: 8847–8851. PMID: [1528901](#)
4. Stanway G, Hyypia T. Parechoviruses. *J Virol*. 1999; 73: 5249–5254. PMID: [10364270](#)
5. Al-Sunaidi M, Williams CH, Hughes PJ, Schnurr DP, Stanway G. Analysis of a new human parechovirus allows the definition of parechovirus types and the identification of RNA structural domains. *J Virol*. 2007; 81: 1013–1021. PMID: [17005640](#)
6. Benschop KS, Schinkel J, Luken ME, van den Broek PJ, Beersma MF, Menelik N, et al. Fourth human parechovirus serotype. *Emerg Infect Dis*. 2006; 12: 1572–1575. PMID: [17176575](#)
7. Abed Y, Boivin G. Molecular characterization of a Canadian human parechovirus (HPeV)-3 isolate and its relationship to other HPeVs. *J Med Virol*. 2005; 77: 566–570. PMID: [16254961](#)

8. Drexler JF, Grywna K, Stocker A, Almeida PS, Medrado-Ribeiro TC, Eschbach-Bludau M, et al. Novel human parechovirus from Brazil. *Emerg Infect Dis.* 2009; 15: 310–313. PMID: [19193281](#)
9. Harvala H, Simmonds P. Human parechoviruses: biology, epidemiology and clinical significance. *J Clin Virol.* 2009; 45: 1–9. doi: [10.1016/j.jcv.2009.03.009](#) PMID: [19372062](#)
10. Ito M, Yamashita T, Tsuzuki H, Takeda N, Sakae K. Isolation and identification of a novel human parechovirus. *J Gen Virol.* 2004; 85: 391–398. PMID: [14769896](#)
11. Li L, Victoria J, Kapoor A, Naeem A, Shaikat S, Sharif S, et al. Genomic characterization of novel human parechovirus type. *Emerg Infect Dis.* 2009; 15: 288–291. PMID: [19193275](#)
12. Oberste MS, Maher K, Pallansch MA. Complete sequence of echovirus 23 and its relationship to echovirus 22 and other human enteroviruses. *Virus Res.* 1998; 56: 217–223. PMID: [9783471](#)
13. Watanabe K, Oie M, Higuchi M, Nishikawa M, Fujii M. Isolation and characterization of novel human parechovirus from clinical samples. *Emerg Infect Dis.* 2007; 13: 889–895. PMID: [17553229](#)
14. Benschop K, Thomas X, Serpenti C, Molenkamp R, Wolthers K. High prevalence of human Parechovirus (HPeV) genotypes in the Amsterdam region and identification of specific HPeV variants by direct genotyping of stool samples. *J Clin Microbiol.* 2008; 46: 3965–3970. doi: [10.1128/JCM.01379-08](#) PMID: [18945833](#)
15. Ghazi F, Hughes PJ, Hyypia T, Stanway G. Molecular analysis of human parechovirus type 2 (formerly echovirus 23). *J Gen Virol.* 1998; 79 (Pt 11): 2641–2650. PMID: [9820139](#)
16. Ehrnst A, Eriksson M. Epidemiological features of type 22 echovirus infection. *Scand J Infect Dis.* 1993; 25: 275–281. PMID: [8362222](#)
17. Grist NR, Bell EJ, Assaad F. Enteroviruses in human disease. *Prog Med Virol.* 1978; 24: 114–157. PMID: [360295](#)
18. Joki-Korpela P, Hyypia T. Diagnosis and epidemiology of echovirus 22 infections. *Clin Infect Dis.* 1998; 27: 129–136. PMID: [9675466](#)
19. Tauriainen S, Martiskainen M, Oikarinen S, Lonnrot M, Viskari H, Ilonen J, et al. Human parechovirus 1 infections in young children—no association with type 1 diabetes. *J Med Virol.* 2007; 79: 457–462. PMID: [17311340](#)
20. WIGAND R, SABIN AB. Properties of ECHO types 22, 23 and 24 viruses. *Arch Gesamte Virusforsch.* 1961; 11: 224–247. PMID: [13785166](#)
21. Koskiniemi M, Paetau R, Linnavuori K. Severe encephalitis associated with disseminated echovirus 22 infection. *Scand J Infect Dis.* 1989; 21: 463–466. PMID: [2587949](#)
22. Esposito S, Rahamat-Langendoen J, Ascolese B, Senatore L, Castellazzi L, Niesters HG. Pediatric parechovirus infections. *J Clin Virol.* 2014; 60: 84–89. doi: [10.1016/j.jcv.2014.03.003](#) PMID: [24690382](#)
23. Stanway G, Kalkkinen N, Roivainen M, Ghazi F, Khan M, Smyth M, et al. Molecular and biological characteristics of echovirus 22, a representative of a new picornavirus group. *J Virol.* 1994; 68: 8232–8238. PMID: [7966616](#)
24. Adams MJ, King AM, Carstens EB. Ratification vote on taxonomic proposals to the International Committee on Taxonomy of Viruses (2013). *Arch Virol.* 2013; 158: 2023–2030. doi: [10.1007/s00705-013-1688-5](#) PMID: [23580178](#)
25. Knowles NJ, Hovi T, Hyypia T, King AMQ, Lindberg AM, Pallansch MA, et al. Picornaviridae. In: King AMQ, Adams MJ, Carstens EB, Lefkowitz E, editors. *Virus Taxonomy: Classification and Nomenclature of Viruses: Ninth Report of the International Committee on Taxonomy of Viruses.* Elsevier; 2012. pp. 855–880.
26. Merilahti P, Koskinen S, Heikkila O, Karelehto E, Susi P. Endocytosis of integrin-binding human picornaviruses. *Adv Virol.* 2012; 2012: 547530. doi: [10.1155/2012/547530](#) PMID: [23227048](#)
27. Pulli T, Koivunen E, Hyypia T. Cell-surface interactions of echovirus 22. *J Biol Chem.* 1997; 272: 21176–21180. PMID: [9261123](#)
28. Seitsonen J, Susi P, Heikkila O, Sinkovits RS, Laurinmaki P, Hyypia T, et al. Interaction of  $\alpha\beta 3$  and  $\alpha\beta 6$  integrins with human parechovirus 1. *J Virol.* 2010; 84: 8509–8519. doi: [10.1128/JVI.02176-09](#) PMID: [20554778](#)
29. Triantafilou K, Triantafilou M, Takada Y, Fernandez N. Human parechovirus 1 utilizes integrins  $\alpha\beta 3$  and  $\alpha\beta 1$  as receptors. *J Virol.* 2000; 74: 5856–5862. PMID: [10846065](#)
30. Chang KH, Auvinen P, Hyypia T, Stanway G. The nucleotide sequence of coxsackievirus A9; implications for receptor binding and enterovirus classification. *J Gen Virol.* 1989; 70 (Pt 12): 3269–3280. PMID: [2558158](#)
31. Hughes PJ, Horsnell C, Hyypia T, Stanway G. The coxsackievirus A9 RGD motif is not essential for virus viability. *J Virol.* 1995; 69: 8035–8040. PMID: [7494317](#)

32. Heikkilä O, Susi P, Tevaluoto T, Harma H, Marjomaki V, Hyypia T, et al. Internalization of coxsackievirus A9 is mediated by  $\beta 2$ -microglobulin, dynamin, and Arf6 but not by caveolin-1 or clathrin. *J Virol*. 2010; 84: 3666–3681. doi: [10.1128/JVI.01340-09](https://doi.org/10.1128/JVI.01340-09) PMID: [20089652](https://pubmed.ncbi.nlm.nih.gov/20089652/)
33. Boonyakiat Y, Hughes PJ, Ghazi F, Stanway G. Arginine-glycine-aspartic acid motif is critical for human parechovirus 1 entry. *J Virol*. 2001; 75: 10000–10004. PMID: [11559835](https://pubmed.ncbi.nlm.nih.gov/11559835/)
34. Merilahti P, Karelehto E, Susi P. Role of Heparan Sulfate in Cellular Infection of Integrin-Binding Coxsackievirus A9 and Human Parechovirus 1 Isolates. *PLoS One*. 2016; 11: e0147168. doi: [10.1371/journal.pone.0147168](https://doi.org/10.1371/journal.pone.0147168) PMID: [26785353](https://pubmed.ncbi.nlm.nih.gov/26785353/)
35. Gimond C, van Der Flier A, van Delft S, Brakebusch C, Kuikman I, Collard JG, et al. Induction of cell scattering by expression of beta1 integrins in beta1-deficient epithelial cells requires activation of members of the rho family of GTPases and downregulation of cadherin and catenin function. *J Cell Biol*. 1999; 147: 1325–1340. PMID: [10601344](https://pubmed.ncbi.nlm.nih.gov/10601344/)
36. Hendry E, Hatanaka H, Fry E, Smyth M, Tate J, Stanway G, et al. The crystal structure of coxsackievirus A9: new insights into the uncoating mechanisms of enteroviruses. *Structure*. 1999; 7: 1527–1538. PMID: [10647183](https://pubmed.ncbi.nlm.nih.gov/10647183/)
37. Joki-Korpela P, Marjomaki V, Krogerus C, Heino J, Hyypia T. Entry of human parechovirus 1. *J Virol*. 2001; 75: 1958–1967. PMID: [11160695](https://pubmed.ncbi.nlm.nih.gov/11160695/)
38. Joki-Korpela P, Roivainen M, Lankinen H, Poyry T, Hyypia T. Antigenic properties of human parechovirus 1. *J Gen Virol*. 2000; 81: 1709–1718. PMID: [10859376](https://pubmed.ncbi.nlm.nih.gov/10859376/)
39. Pulli T, Roivainen M, Hovi T, Hyypia T. Induction of neutralizing antibodies by synthetic peptides representing the C terminus of coxsackievirus A9 capsid protein VP1. *J Gen Virol*. 1998; 79 (Pt 9): 2249–2253. PMID: [9747735](https://pubmed.ncbi.nlm.nih.gov/9747735/)
40. Kankaanpää P, Paavolainen L, Tiitta S, Karjalainen M, Paivarinne J, Nieminen J, et al. BiImageXD: an open, general-purpose and high-throughput image-processing platform. *Nat Methods*. 2012; 9: 683–689. doi: [10.1038/nmeth.2047](https://doi.org/10.1038/nmeth.2047) PMID: [22743773](https://pubmed.ncbi.nlm.nih.gov/22743773/)
41. Upla P, Marjomaki V, Kankaanpää P, Ivaska J, Hyypia T, Van Der Goot FG, et al. Clustering induces a lateral redistribution of alpha 2 beta 1 integrin from membrane rafts to caveolae and subsequent protein kinase C-dependent internalization. *Mol Biol Cell*. 2004; 15: 625–636. PMID: [14657242](https://pubmed.ncbi.nlm.nih.gov/14657242/)
42. Jokinen J, White DJ, Salmela M, Huhtala M, Kapyla J, Sipila K, et al. Molecular mechanism of alpha2-beta1 integrin interaction with human echovirus 1. *EMBO J*. 2010; 29: 196–208.
43. Heikkilä O, Susi P, Stanway G, Hyypia T. Integrin  $\alpha\text{V}\beta 6$  is a high-affinity receptor for coxsackievirus A9. *J Gen Virol*. 2009; 90: 197–204. doi: [10.1099/vir.0.004838-0](https://doi.org/10.1099/vir.0.004838-0) PMID: [19088289](https://pubmed.ncbi.nlm.nih.gov/19088289/)
44. Triantafilou K, Triantafilou M. A biochemical approach reveals cell-surface molecules utilised by Picornaviridae: Human Parechovirus 1 and Echovirus 1. *J Cell Biochem*. 2001; 80: 373–381. PMID: [11135368](https://pubmed.ncbi.nlm.nih.gov/11135368/)
45. Williams CH, Kajander T, Hyypia T, Jackson T, Sheppard D, Stanway G. Integrin  $\alpha\text{v}\beta 6$  is an RGD-dependent receptor for coxsackievirus A9. *J Virol*. 2004; 78: 6967–6973. PMID: [15194773](https://pubmed.ncbi.nlm.nih.gov/15194773/)
46. Zhang Z, Morla AO, Vuori K, Bauer JS, Juliano RL, Ruoslahti E. The  $\alpha\text{v}\beta 1$  integrin functions as a fibronectin receptor but does not support fibronectin matrix assembly and cell migration on fibronectin. *J Cell Biol*. 1993; 122: 235–242. PMID: [8314844](https://pubmed.ncbi.nlm.nih.gov/8314844/)
47. Bazzoni G, Ma L, Blue ML, Hemler ME. Divalent cations and ligands induce conformational changes that are highly divergent among beta1 integrins. *J Biol Chem*. 1998; 273: 6670–6678. PMID: [9506964](https://pubmed.ncbi.nlm.nih.gov/9506964/)
48. Davison E, Diaz RM, Hart IR, Santis G, Marshall JF. Integrin  $\alpha 5\beta 1$ -mediated adenovirus infection is enhanced by the integrin-activating antibody TS2/16. *J Virol*. 1997; 71: 6204–6207. PMID: [9223518](https://pubmed.ncbi.nlm.nih.gov/9223518/)
49. Dibya D, Arora N, Smith EA. Noninvasive measurements of integrin microclustering under altered membrane cholesterol levels. *Biophys J*. 2010; 99: 853–861. doi: [10.1016/j.bpj.2010.05.027](https://doi.org/10.1016/j.bpj.2010.05.027) PMID: [20682263](https://pubmed.ncbi.nlm.nih.gov/20682263/)
50. Manders EMM, Verbeek FJ, Aten JA. Measurement of co-localization of objects in dual-colour confocal images. *J Microsc*. 1993; 169: 375–382.
51. Danen EH, Sonneveld P, Brakebusch C, Fassler R, Sonnenberg A. The fibronectin-binding integrins  $\alpha 5\beta 1$  and  $\alpha\text{v}\beta 3$  differentially modulate RhoA-GTP loading, organization of cell matrix adhesions, and fibronectin fibrillogenesis. *J Cell Biol*. 2002; 159: 1071–1086. PMID: [12486108](https://pubmed.ncbi.nlm.nih.gov/12486108/)
52. Gavrilovskaya IN, Shepley M, Shaw R, Ginsberg MH, Mackow ER.  $\beta 3$  Integrins mediate the cellular entry of hantaviruses that cause respiratory failure. *Proc Natl Acad Sci U S A*. 1998; 95: 7074–7079. PMID: [9618541](https://pubmed.ncbi.nlm.nih.gov/9618541/)
53. Gavrilovskaya IN, Brown EJ, Ginsberg MH, Mackow ER. Cellular entry of hantaviruses which cause hemorrhagic fever with renal syndrome is mediated by  $\beta 3$  integrins. *J Virol*. 1999; 73: 3951–3959. PMID: [10196290](https://pubmed.ncbi.nlm.nih.gov/10196290/)
54. Mackow ER, Gavrilovskaya IN. Cellular receptors and hantavirus pathogenesis. *Curr Top Microbiol Immunol*. 2001; 256: 91–115. PMID: [11217408](https://pubmed.ncbi.nlm.nih.gov/11217408/)



55. Raymond T, Gorbunova E, Gavrilovskaya IN, Mackow ER. Pathogenic hantaviruses bind plexin-semaphorin-integrin domains present at the apex of inactive, bent  $\alpha\text{V}\beta 3$  integrin conformers. *Proc Natl Acad Sci U S A*. 2005; 102: 1163–1168. PMID: [15657120](#)
56. Jackson T, Mould AP, Sheppard D, King AM. Integrin  $\alpha\text{V}\beta 1$  is a receptor for foot-and-mouth disease virus. *J Virol*. 2002; 76: 935–941. PMID: [11773368](#)
57. Feire AL, Koss H, Compton T. Cellular integrins function as entry receptors for human cytomegalovirus via a highly conserved disintegrin-like domain. *Proc Natl Acad Sci U S A*. 2004; 101: 15470–15475. PMID: [15494436](#)
58. Kowalik TF, Wing B, Haskill JS, Azizkhan JC, Baldwin AS Jr, Huang ES. Multiple mechanisms are implicated in the regulation of NF- $\kappa$ B activity during human cytomegalovirus infection. *Proc Natl Acad Sci U S A*. 1993; 90: 1107–1111. PMID: [8381532](#)
59. Wang X, Huang DY, Huang SM, Huang ES. Integrin  $\alpha\text{V}\beta 3$  is a coreceptor for human cytomegalovirus. *Nat Med*. 2005; 11: 515–521. PMID: [15834425](#)
60. Li E, Stupack D, Klemke R, Cheresh DA, Nemerow GR. Adenovirus endocytosis via  $\alpha\text{V}$  integrins requires phosphoinositide-3-OH kinase. *J Virol*. 1998; 72: 2055–2061. PMID: [9499060](#)
61. Philpott NJ, Nociari M, Elkon KB, Falck-Pedersen E. Adenovirus-induced maturation of dendritic cells through a PI3 kinase-mediated TNF- $\alpha$  induction pathway. *Proc Natl Acad Sci U S A*. 2004; 101: 6200–6205. PMID: [15071185](#)
62. Rajala MS, Rajala RV, Astley RA, Butt AL, Chodosh J. Corneal cell survival in adenovirus type 19 infection requires phosphoinositide 3-kinase/Akt activation. *J Virol*. 2005; 79: 12332–12341. PMID: [16160160](#)
63. Veetil MV, Sharma-Walia N, Sadagopan S, Raghu H, Sivakumar R, Naranatt PP, et al. RhoA-GTPase facilitates entry of Kaposi's sarcoma-associated herpesvirus into adherent target cells in a Src-dependent manner. *J Virol*. 2006; 80: 11432–11446. PMID: [17005646](#)
64. Krishnan HH, Sharma-Walia N, Streblov DN, Naranatt PP, Chandran B. Focal adhesion kinase is critical for entry of Kaposi's sarcoma-associated herpesvirus into target cells. *J Virol*. 2006; 80: 1167–1180. PMID: [16414994](#)
65. Huttunen M, Waris M, Kajander R, Hyypia T, Marjomaki V. Coxsackievirus A9 infects cells via nonacidic multivesicular bodies. *J Virol*. 2014; 88: 5138–5151. doi: [10.1128/JVI.03275-13](#) PMID: [24574401](#)
66. Koistinen P, Heino J. The selective regulation of  $\alpha\text{V}\beta 1$  integrin expression is based on the hierarchical formation of  $\alpha\text{V}$ -containing heterodimers. *J Biol Chem*. 2002; 277: 24835–24841. PMID: [11997396](#)
67. Lord R, Parsons M, Kirby I, Beavil A, Hunt J, Sutton B, et al. Analysis of the interaction between RGD-expressing adenovirus type 5 fiber knob domains and  $\alpha\text{V}\beta 3$  integrin reveals distinct binding profiles and intracellular trafficking. *J Gen Virol*. 2006; 87: 2497–2505. PMID: [16894187](#)
68. Izmailyan R, Hsao JC, Chung CS, Chen CH, Hsu PW, Liao CL, et al. Integrin  $\beta 1$  mediates vaccinia virus entry through activation of PI3K/Akt signaling. *J Virol*. 2012; 86: 6677–6687. doi: [10.1128/JVI.06860-11](#) PMID: [22496232](#)
69. Stewart PL, Nemerow GR. Cell integrins: commonly used receptors for diverse viral pathogens. *Trends Microbiol*. 2007; 15: 500–507. PMID: [17988871](#)
70. Cseke G, Maginnis MS, Cox RG, Tollefson SJ, Podsiad AB, Wright DW, et al. Integrin  $\alpha\text{V}\beta 1$  promotes infection by human metapneumovirus. *Proc Natl Acad Sci U S A*. 2009; 106: 1566–1571. doi: [10.1073/pnas.0801433106](#) PMID: [19164533](#)
71. Li E, Brown SL, Stupack DG, Puente XS, Cheresh DA, Nemerow GR. Integrin  $\alpha\text{V}\beta 1$  is an adenovirus coreceptor. *J Virol*. 2001; 75: 5405–5409. PMID: [11333925](#)
72. Croyle MA, Walter E, Janich S, Roessler BJ, Amidon GL. Role of integrin expression in adenovirus-mediated gene delivery to the intestinal epithelium. *Hum Gene Ther*. 1998; 9: 561–573. PMID: [9525317](#)
73. Kasono K, Blackwell JL, Douglas JT, Dmitriev I, Strong TV, Reynolds P, et al. Selective gene delivery to head and neck cancer cells via an integrin targeted adenoviral vector. *Clin Cancer Res*. 1999; 5: 2571–2579. PMID: [10499635](#)
74. Dedhar S, Gray V. Isolation of a novel integrin receptor mediating Arg-Gly-Asp-directed cell adhesion to fibronectin and type I collagen from human neuroblastoma cells. Association of a novel  $\beta 1$ -related subunit with  $\alpha\text{V}$ . *J Cell Biol*. 1990; 110: 2185–2193. PMID: [1693626](#)
75. Friedlander DR, Zagzag D, Shiff B, Cohen H, Allen JC, Kelly PJ, et al. Migration of brain tumor cells on extracellular matrix proteins in vitro correlates with tumor type and grade and involves  $\alpha\text{V}$  and  $\beta 1$  integrins. *Cancer Res*. 1996; 56: 1939–1947. PMID: [8620517](#)
76. Meyer T, Marshall JF, Hart IR. Expression of  $\alpha\text{V}$  integrins and vitronectin receptor identity in breast cancer cells. *Br J Cancer*. 1998; 77: 530–536. PMID: [9484807](#)